Solubility Measurement and Modeling of Methane in Methanol and Ethanol Aqueous Solutions

Solubility Measurement and Modeling of Methane in Methanol and Ethanol Aqueous Solutions

Michael Wise, Antonin Chapoy, Rod Burgass*

Hydrates, Flow Assurance & Phase Equilibria, Institute of Petroleum Engineering, Heriot Watt University, EH14 4AS

Abstract

Hydrate formation is a major flow assurance issue in the petroleum industry and the knowledge of hydrate inhibitor distribution is essential for the economic gas transportation and processing operation. A number of measurements were made to determine the solubility of methane, the main constituent in natural gas, in methanol and ethanol aqueous solutions. The results showed that the addition of water significantly reduces the solubility in methanol and ethanol Methanol and ethanol are two of the most commonly used gas hydrate inhibitors in the petroleum industry. The solubility data are important in developing binary interaction parameters used in predicting inhibitor distribution in multi-component systems containing water. To fill the significant gap in the open literature data the solubility of methane in 70 and 50 wt% methanol and ethanol solutions at 273.15 to 298.15 K and 0.46 to 44 MPa were measured. The average repeatability of the experimental results was calculated to be 2.5%. The results from this work and literature were used to optimize the interaction parameters of the CPA-SRK72 equation of state. The model calculations using a single variable Binary Interaction Parameter was able to reproduce the new experimental results with a significant increase in accuracy.

Keywords

Gas Hydrates, Inhibitor Distribution, High Pressure, Low Temperature, Water

Introduction

The world's hunger for energy is driving the petroleum industry to explore less accessible sources, resulting in dramatic changes in the petroleum industry. These changes have been amplified by the development in deep-water exploration technologies. Although this has recently reduced due to the glut in production and low oil prices. Some industry experts believe that as drilling stalls and many hydraulic fracking companies declare bankruptcy, the overproduction will likely decrease resulting in a slow resurgence of demand to accommodate the ever increasing population of the planet. This will lead the petroleum industry to continue exploiting the more inaccessible locations.

Flow assurance has become a key field in this ever changing environment, ensuring un-interrupted production and transport of gas to the processing facilities. Hydrate formation is one of the biggest flow assurance problems faced by the industry at the deep sea facility's operating conditions. Thermodynamic inhibitors such as methanol, ethanol and Mono-ethylene glycol (MEG) are commonly used to prevent hydrate formation. These are water soluble chemicals and reduce the water activity, hence shifting the hydrate phase boundary to lower temperatures and higher pressures. Hydrate inhibitor injection entails substantial Capital Expenditure (CAPEX) and Operating Expenditure (OPEX) thus it is essential for operators to be able to make accurate calculations using their thermodynamic models. Therefore, this study focused on solubility measurement and modeling of methane (CH_4) in methanol and ethanol aqueous solutions. This paper follows up on the work published earlier by the authors measuring and modelling the solubility of CH_4 in pure methanol and ethanol. [1] These measurements were used to optimize the Binary Interaction Parameters (BIP) between methane and the alcohols. BIPs are essential for developing thermodynamic models capable of predicting inhibitor distribution in multi-component

systems. The data from this work may be used to develop BIPs and optimize the classical and statistical models used by operators.

Wang et al. [2] conducted the most comprehensive investigation into the solubility of methane in methanol solutions at 5.05 – 40.05 MPa and 283.2 – 303.2 K in 20 – 100 wt% methanol solutions. Yarym-agaev et al. conducted a number of solubility measurements for CH_4 in methanol at 298.15 to 338.15 K and 2.5 to 12.5 MPa. [3] Brunner et al. completed one the most extensive studies of CH_4 solubility in methanol and methanol rich CH_4 (vapor phase) with measurements at 298.15 to 373.15 K and 3 to 100 MPa. [4] Hong et al. also made a similar significant contribution to solubility data for methanol in CH_4 making measurements between 200 to 330 K and 0.6 to 41.3 MPa. [5] Schneider measured the solubility of CH_4 in methanol in his PhD thesis at 183.15 to 298.15 and 0.9 to 10.3 MPa. [6] Ukai et al. measured CH_4 in methanol solubility at 280.15 K and the pressure ranges of 2.1 to 11.4 MPa. [7] Frost et al. also made a number of measurements recently at 298.87 K and 5 to 18 MPa. [8]

The solubility data for CH_4 in ethanol at high pressure in the open literature is very limited. The authors were unable to obtain any CH_4 in ethanol solution solubility data in the open literature. Suzuki et al. made a limited number of measurements at 313.4 to 333.4 K and 1.8 to 10.5 MPa. [9] Brunner et al. made a number of measurements at 298.15 to 498.15 K and 3.3 to 31.5 MPa. [10] Ukai et al. made measurements at 280.15 K and 1.5 to 5.7 MPa. [7] Friend et al. also made measurements at 323 to 373 K and 2.1 to 2.7 MPa. [11]

As clearly apparent from the literature review, the availability of solubility data for CH_4 in methanol and ethanol aqueous solutions in open literature is extremely limited. Thus this study's main focus was the measurement and modeling of CH_4 in methanol and ethanol solutions at low temperatures and a wide range of pressures. Ethanol is particularly important in the modern

petroleum industry where there is a move towards the use of greener, less toxic chemicals. It is also of interest to petroleum companies operating in South America where significant amounts of ethanol are produced making its use far more economically viable than other inhibitors. [12–15]

Materials and Method

The details of the materials used are detailed in Table 1.

Table 1 Materials, their purity and suppliers used.

Chemical Name	Source	Mole Fraction Purity[a]	Purity Certification	Analysis method[b]
Methanol	J.T. Baker	0.9980	Avantor Materials	GC
Ethanol	J.T. Baker	0.9990	Avantor Materials	GC
Methane	BOC	0.9999	BOC Certified	GC
Deionized Water	Pure Lab Elga 2	-	-	-

[a] No additional purification is carried out for all samples. [b] GC: Gas Chromatography

The setup used in this work was the same as the rocking cell setup used by Chapoy et al. [16] to determine the saturation pressure of a multicomponent mixtures. The setup used in these measurements has been described in previous publications. [1,17]

A high pressure rocking cell was used to measure the solubility of CH_4 in alcohol solutions at various pressures and isotherms at equilibrium. A liquid sample was flashed at each pressure and the volume of gas and mass of liquid was measured. These were then used to calculate the solubility of methane in the alcohol solution as described by Kapateh et al. [1].

See Eq. 8 in the Appendix for the solubility calculation formula. This process was repeated for all measurements made at the various temperatures and pressures.

The standard uncertainty of the high pressure rocking cell transducer was u(P) = 0.04 MPa and the standard uncertainty for the PRT temperature probe was u(T) = 0.05 K, which had negligible effect on the overall standard uncertainty of the measurements.

Thermodynamic Modeling

The original thermodynamic model utilized in this work has been described in detail elsewhere [18–20]. This section briefly summarizes the CPA-SRK72 EoS used throughout this work to calculate the fugacities of the components in the fluid phases. It is based on the uniformity of fugacity of each component throughout all of the phases.

The Cubic-Plus Association (CPA-SRK72) developed by Kontogeorgis et al. [21] combining the original SRK EoS developed by Soave [22] and an associating term.

Eq. 1 expresses the CPA-SRK72 in terms of pressure with the sum of the SRK EoS and the contribution association term published by Michelsen and Hendriks [23]:

$$P = \frac{RT}{V_m - b} - \frac{\alpha(T)}{V_m(V_m + b)} - \frac{1}{2}\left(\frac{RT}{V_m}\right)\left(1 + \frac{1}{V_m}\frac{\partial \ln g}{\partial\left(\frac{1}{V_m}\right)}\right)\sum_i x_i \sum_{A_i}\left(1 - X_{A_i}\right) \quad (1)$$

Where V_m is the molar volume, X_{A_i} is the fraction of A-sites of molecular i that are not bonded with other active sites and x_i is the mole fraction of the component i.

The binary interaction parameters (BIPs) between methane and methanol and ethanol were adjusted using the solubility data mentioned previously (Kapateh et al. [1] and Haghighi et al. [18]) and the new measured data through a Simplex algorithm using the objective function, *OF*, displayed in Eq. 2: [24]

$$OF = \frac{1}{N}\sum_{1}^{N}\left|\frac{x_{\exp} - x_{cal}}{x_{\exp}}\right| \quad (2)$$

Where x is the solubility of methane in methanol/ethanol solution**,** N is the number of data points.

The BIPs between water and methanol were calculated using the correlation shown in Eq. 3 developed by Haghighi. [25] Eq. 4 was used to calculate the BIPs between water and ethanol, and Eq. 5 was used to calculate the BIPs between methane and water, which were developed by the same author.

$$k_{ij} = 3.4463\times10^{-6}T^2 - 9.5986\times10^{-4}T - 0.1197 \quad (3)$$

$$k_{ij} = -5.6946\times10^{-7}T^3 + 4.9661\times10^{-4}T^2 - 0.1412\times T - 13.0024 \quad (4)$$

$$k_{ij} = 0.8613 + \frac{-251.0540}{T} \quad (5)$$

Results and Discussion

Table 2 shows the measured solubility of methane in 70 wt% methanol aqueous solution, where T is temperature in Kelvin, P is the pressure in MPa and x_i is the moles of CH_4 in the alcohol.

Table 3 and Table 4 show the solubility of methane in 70 and 50 wt% ethanol solutions respectively. Figure 1 shows the solubility of methane in 70wt% methanol solution together with model correlations utilizing the BIPs developed based on the binary and tertiary data respectively. The model was tuned using a single BIP between methane and methanol for the dataset as demonstrated in Table 5 and the data presented by Wang et al. [2] shown in Table 6. The CPA-SRK72 model correlations using the new methane-methanol BIP showed an overall absolute average deviation of 20.7%, however it is important to note the largest deviation can be seen at the lower pressures.

Table 7 shows the BIPs between methane and ethanol for pure, [1] 70 and 50 wt% ethanol solution. Figure 2 and Figure 3 show the solubility of methane in 70 and 50 wt% ethanol solution respectively. Figure 2 shows the solubility for methane in ethanol at 273.15 and 298.15 K. Using the concentration dependent regressed, the CPA-SRK72 correlations showed and overall absolute average deviation of 10.1% over the data range.

The solubility measurements demonstrated in Figure 3 for 50 wt% ethanol solutions showed a similar inflection point at 10 MPa, which was not produced by the optimized (k_{ij} = 0.130) CPA-SRK72 model calculations. However, the optimized models demonstrated significant improvement in reducing the correlation deviation especially at higher pressures, showing an overall absolute deviation of 21.0%. This methodology has been discussed in details by Wise and Chapoy for systems containing TEG solutions. [17]

Figure 4 illustrates the optimized concentration dependent BIPs between methanol and methane regressed using the data presented by Wang et al. [2] and measurements in this work. Figure 5 shows the optimized k_{ij} BIPs developed using the experimental measurements from this work at various ethanol concentrations.

Using the data presented by Wang et al. [2] a correlation was developed which can be used to calculate concentration dependent (methanol) BIPs between methane and methanol for systems containing water (Eq. 6). Figure 6 shows the bubble point measurements for a quartinary system containing decane, methane, methanol and water. The bubble points were calculated by CPA-SRK72 using the k_{ij} developed by Haghighi et al. [18] and the k_{ij} calculated utilizing the correlation developed using the data published by Wang et al. [2]. As can be clearly seen, the calculations significantly improve using the k_{ij} calculated from Eq. 6.

A similar correlation was developed using the data from this work which can be utilized to calculate concentration (ethanol) dependent BIPs between methane and ethanol (Eq. 7). The BIPs fit into a quadratic, thus it is possibly to predict accurate k_{ij} values using the equation demonstrated for 50 – 100 wt% ethanol solutions (Eq. 7).

Table 2. Experimental Mole Fraction Solubilities *xi* of Methane in Methanol + Water Solution (w(methanol) = 0.70) at Temperature T and various pressures P and Standard Uncertainty for Each Measurement *u(x)*[a].

T/K	*P*/MPa	x_i (mol frac)	$u(x_i)$
293.15	0.54	0.0023	0.0001
293.15	0.54	0.0021	0.0001
293.15	0.60	0.0028	0.0001
293.15	0.61	0.0027	0.0001
293.15	1.51	0.0049	0.0002
293.15	1.52	0.0046	0.0001
293.15	2.49	0.0067	0.0002
293.15	2.49	0.0071	0.0002
293.15	4.32	0.0100	0.0003
293.15	4.34	0.0099	0.0003
293.15	6.54	0.0134	0.0004
293.15	10.33	0.0188	0.0005
293.15	10.33	0.0192	0.0005
293.15	18.88	0.0265	0.0007
293.15	26.43	0.0320	0.0009
293.15	26.52	0.0322	0.0009
293.15	35.35	0.0363	0.0010

[a] Standard uncertainties u are u(T) = 0.05 K, u(P) = 0.04 MPa, and u(w) = 0.0001.

Table 3. Experimental Mole Fraction Solubilities *xi* of Methane in Ethanol + Water Solution (w(ethanol) = 0.70) at Temperature T and various pressures P and Standard Uncertainty for Each Measurement *u(x)*[a].

T/K	*P*/MPa	x_i (mol frac)	$u(x_i)$
273.15	0.97	0.0026	0.0001
273.15	1.00	0.0027	0.0001
273.15	4.56	0.0067	0.0002
273.15	4.61	0.0065	0.0002
273.15	9.34	0.0222	0.0006
273.15	9.36	0.0218	0.0006
273.15	16.43	0.0529	0.0014
273.15	16.44	0.0552	0.0015
273.15	23.65	0.0781	0.0020
273.15	23.67	0.0786	0.0020
273.15	30.73	0.0904	0.0023
273.15	30.76	0.0924	0.0024
273.15	37.31	0.0055	0.0002
273.15	37.34	0.0045	0.0002
273.15	43.95	0.0139	0.0004
273.15	43.97	0.0145	0.0004
298.15	0.46	0.0250	0.0007
298.15	0.49	0.0256	0.0007
298.15	2.85	0.0365	0.0010
298.15	2.88	0.0370	0.0010
298.15	7.15	0.0437	0.0012
298.15	7.16	0.0443	0.0012

298.15	13.02	0.0507	0.0013
298.15	13.04	0.0501	0.0013
298.15	19.08	0.0564	0.0015
298.15	19.09	0.0546	0.0014
298.15	26.71	0.0586	0.0015
298.15	26.73	0.0607	0.0016
298.15	34.53	0.0025	0.0001
298.15	34.54	0.0030	0.0001
298.15	41.85	0.0094	0.0003
298.15	41.88	0.0092	0.0003

[a] Standard uncertainties u are u(T) = 0.05 K, u(P) = 0.04 MPa, and u(w) = 0.0001.

Table 4. Experimental Mole Fraction Solubilities *xi* of Methane in Ethanol + Water Solution (w(ethanol) = 0.50) at Temperature T and various pressures P and Standard Uncertainty for Each Measurement *u(x)*[a].

T/K	*P*/MPa	x_i (mol frac)	$u(x_i)$
273.15	0.52	0.0015	0.0001
273.15	0.53	0.0016	0.0001
273.15	1.68	0.0030	0.0001
273.15	1.68	0.0035	0.0001
273.15	2.63	0.0038	0.0001
273.15	2.65	0.0044	0.0001
273.15	4.49	0.0055	0.0002
273.15	4.52	0.0058	0.0002
273.15	8.01	0.0086	0.0002
273.15	8.02	0.0082	0.0002
273.15	13.96	0.0119	0.0003
273.15	13.98	0.0118	0.0003
273.15	20.99	0.0142	0.0004
273.15	21.01	0.0146	0.0004
298.15	0.66	0.0021	0.0001
298.15	0.68	0.0022	0.0001
298.15	1.48	0.0034	0.0001
298.15	1.48	0.0035	0.0001
298.15	3.96	0.0050	0.0001
298.15	3.96	0.0055	0.0002
298.15	6.92	0.0078	0.0002
298.15	13.04	0.0120	0.0003

298.15	13.06	0.0121	0.0003
298.15	19.51	0.0150	0.0004
298.15	19.53	0.0150	0.0004
298.15	28.04	0.0185	0.0005
298.15	34.37	0.0196	0.0005

[a] Standard uncertainties u are u(T) = 0.05 K, u(P) = 0.04 MPa, and u(w) = 0.0001.

Table 5. Optimized BIPs between methane and methanol for pure [18] and methanol aqueous solutions.

Wt% methanol	Mole Fraction	BIPs (k_{ij})	T range (K)
70	0.567	0.099	293.15

Table 6. Optimized BIPs between methane and methanol for pure and methanol aqueous solutions using the data from Wang et al. [2]

Methanol		BIPs (k_{ij})	T range (K)
Wt%	Mole Fraction		
20	0.123	0.273	283.2 - 303.2
40	0.273	0.239	283.2 - 303.2
60	0.457	0.136	283.2 - 303.2
80	0.692	0.058	283.2 - 303.2
100	1	-0.019	283.2 - 303.2

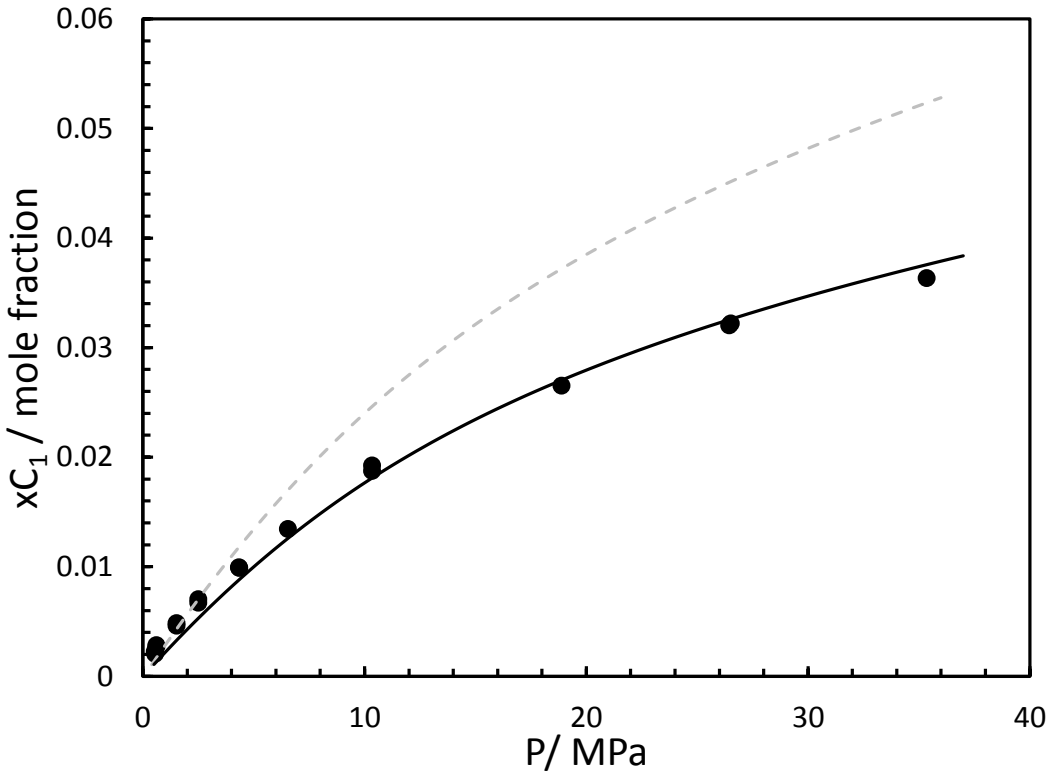

Figure 1. Methane Solubility in 70 wt% methanol solution at (●) 293.15. Lines: CPA-SRK72 model prediction. Grey Dashed Line: k_{ij} = 0.049. Black Line: k_{ij} = 0.099.

Table 7. Optimized BIPs between methane and ethanol for pure and ethanol aqueous solutions.

Ethanol		BIPs (k_{ij})	T range (K)
Wt%	Mole Fraction		
100	1	-0.049	238.15 – 298.15
70	0.477	0.052	273.15 – 298.15
50	0.281	0.130	273.15 – 298.15

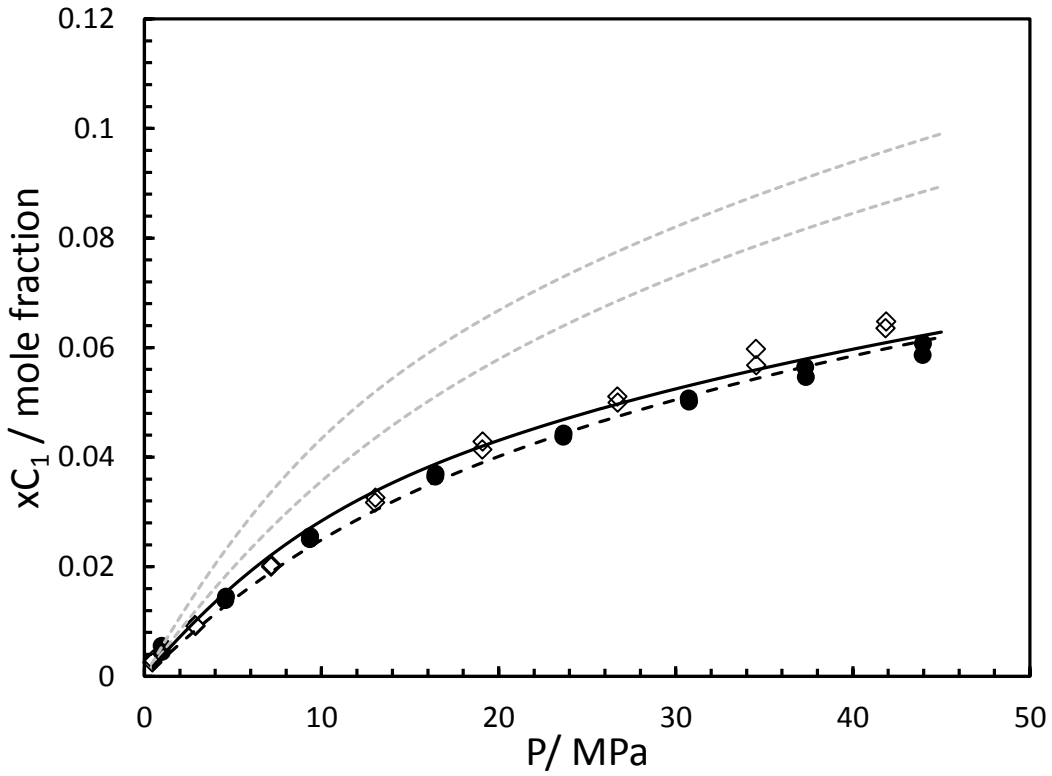

Figure 2. Methane Solubility in 70 wt% ethanol solution at (●) 273.15, (◇) 298.15 K. Line: CPA-SRK72 model predictions. Grey Lines: k_{ij} = -0.049. Black Lines: k_{ij} = 0.052 prediction for 273.15 *K* and 298.15 *K* (respectively – high to low solubility).

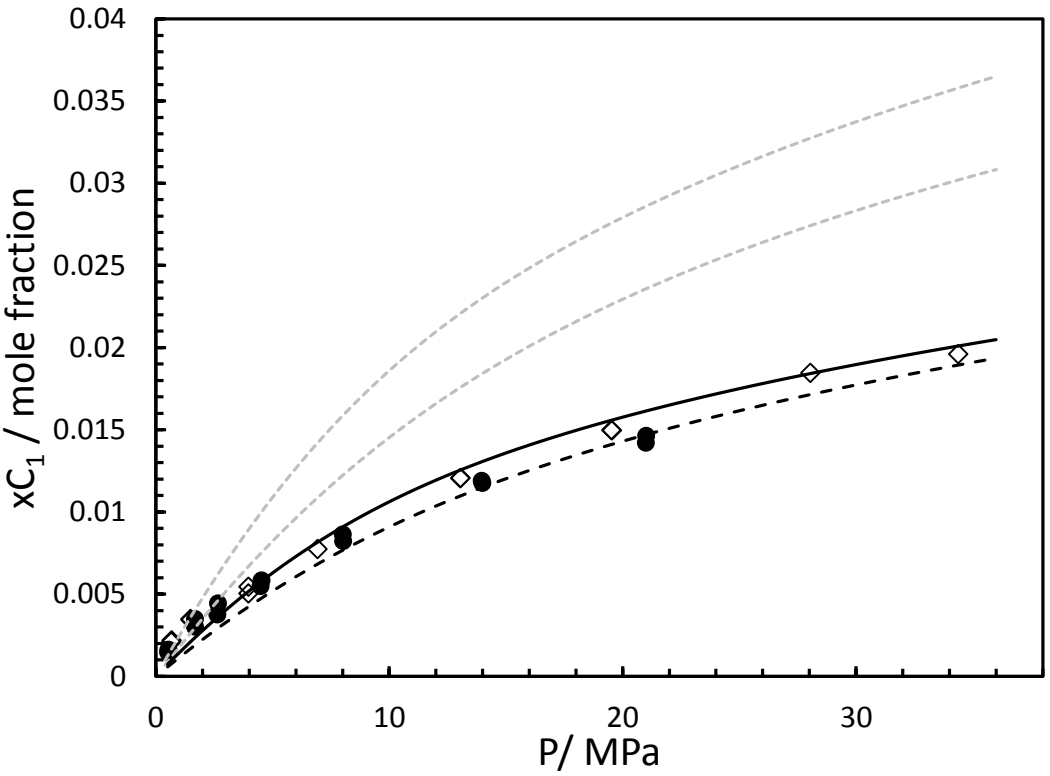

Figure 3. Methane Solubility in 50 wt% ethanol solution at (●) 273.15, (◇) 298.15 K. Lines: CPA-SRK72 model predictions. Dashed Grey Lines: k_{ij} = -0.049. Black Line: k_{ij} = 0.130 prediction for 273.15 *K*. Black Dashed Line: k_{ij} = 0.130 prediction for 298.15 *K*.

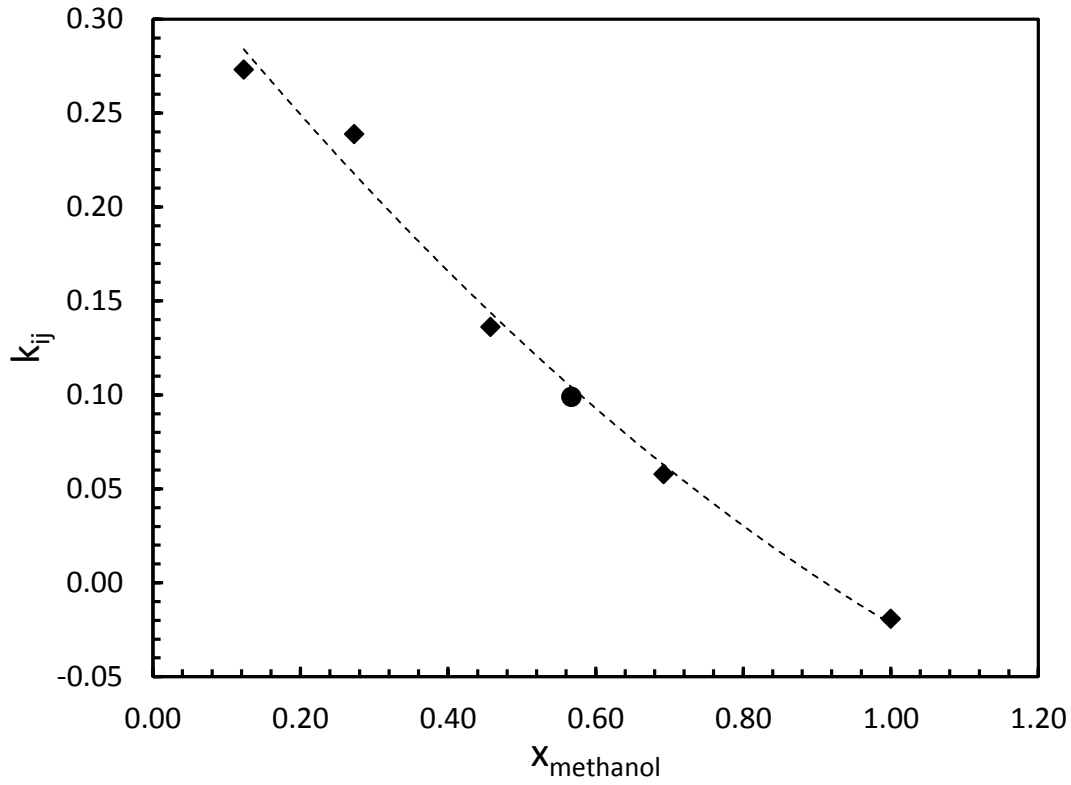

Figure 4. Binary Interaction Parameter, k_{ij} between methane and methanol for pure and aqueous solutions using the work of Wang et al. (◆) [2] and this work (●). Correlation corresponds to the Wang et al. data to ensure independence. [2]

$$k_{ij} = 0.13x^2 - 0.4948x + 0.343 \quad (6)$$

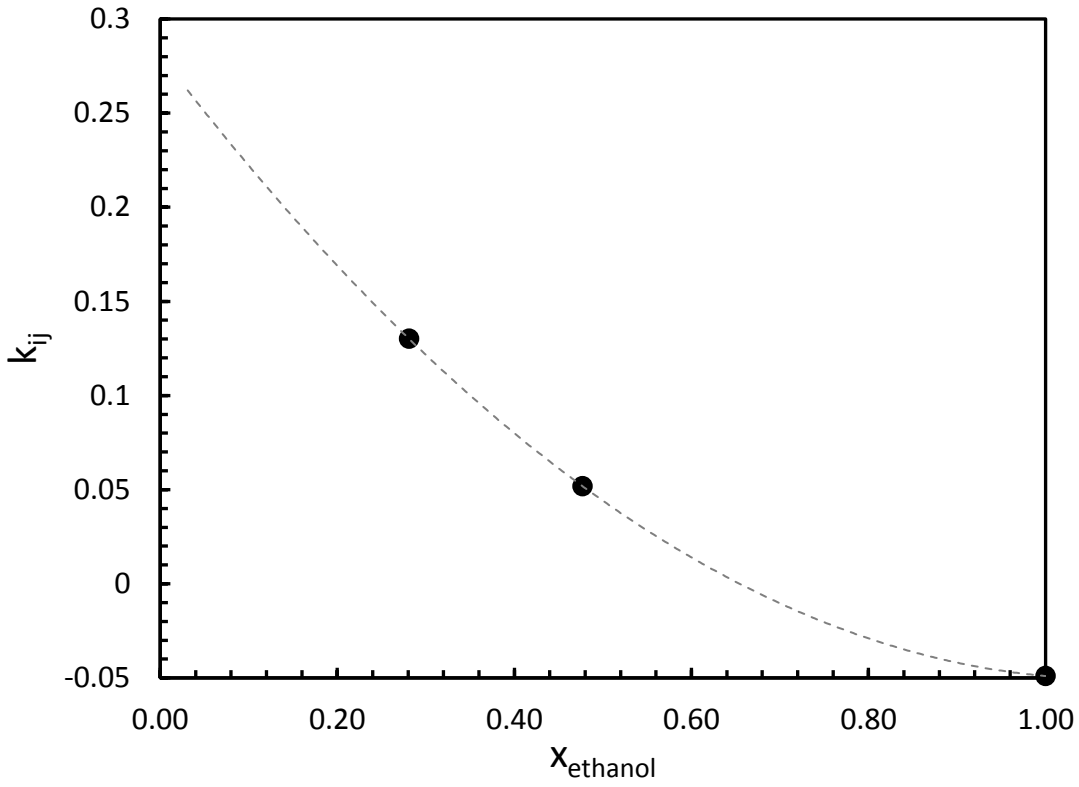

Figure 5. Binary Interaction Parameter, k_{ij} between methane and ethanol for pure and aqueous solutions.

$$k_{ij} = 0.2875x^2 - 0.6175x + 0.281 \quad (7)$$

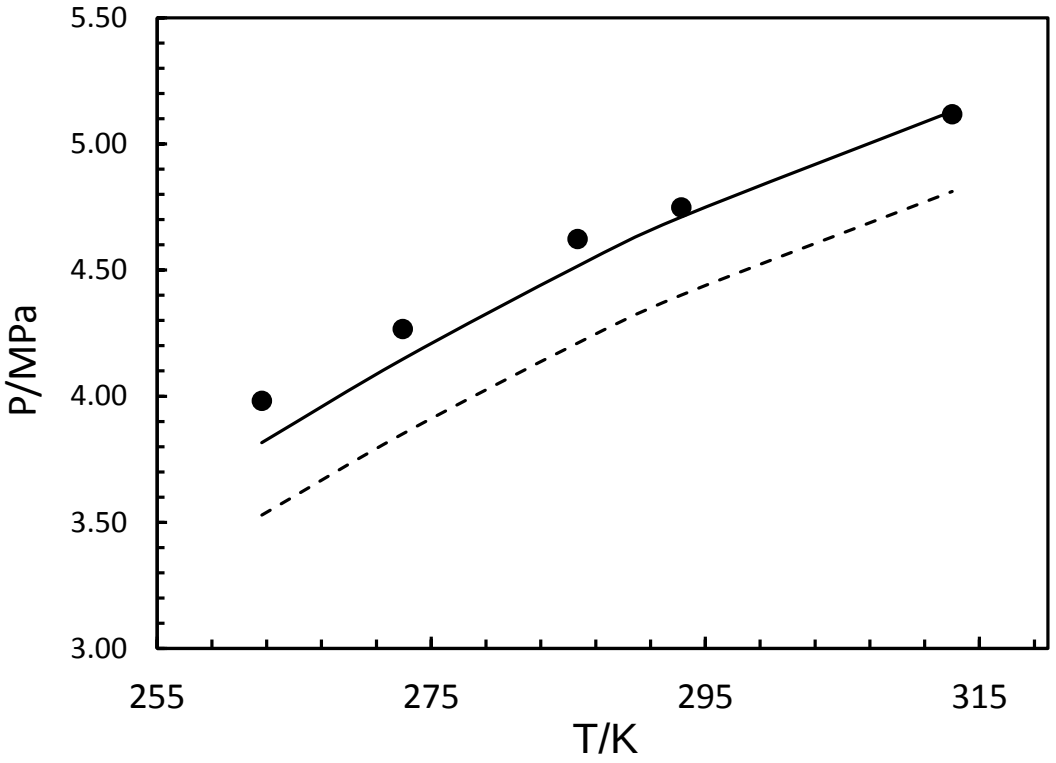

Figure 6. Shows the bubble point measurements for a decane-methane-methanol-water system (●) measured by the authors which (unpublished data). Black line: CPA-SRK72 model prediction with modified k_{ij}. Dashed line: CPA-SRK72 model prediction with original k_{ij}.

Conclusion

The solubility of methane in methanol and ethanol was substantially reduced with the addition of water. This illustrated the affinity of methanol and ethanol molecule surfaces to form hydrogen bonds with water, thus reducing the available surfaces for CH_4 interaction. This had previously been observed by Wang et al. [2] measuring the solubility of CH_4 in methanol solutions.

The model calculations using the BIPs developed for the pure alcohols demonstrated significant deviation from the experimental work, however the model calculations were drastically improved by regressing BIPs between methane and the alcohol using the solubility in aqueous solutions.

It is essential to note that the results from this work were used to optimize the CPA-SRK72 EoS for ethanol solutions, due to the limitation of independent data in the open literature. Both modeling and experimental results can be directly used by the industry and research organizations, however it is important to note to ensure reliability of the model, the results must be compared to independent literature data.

Appendix – Uncertainty Calculations

The nomenclature for the uncertainty calculations are shown in Table 8.

Eq. 8 is used to calculate the solubility of CH_4 in the methanol/ethanol solutions.

$$x_i = \frac{\left[n^v_{CH_4} + n^l_{CH_4}\right] - \left[n^v_{EtOH} - n^v_{water}\right]}{n^l_{EtOH} + n^l_{water} + n^v_{EtOH} + n^v_{CH_4} + n^l_{CH_4} + n^v_{water}} \tag{8}$$

Eq. 9 demonstrates the solubility calculation in respect to the volume measured.

$$x_i = \frac{\left[(v_{CH_4} \times \rho_{CH_4}) + n^l_{CH_4}\right] - \left[n^v_{EtOH} - n^v_{water}\right]}{n^l_{EtOH} + n^l_{water} + n^v_{EtOH} + (v_{CH_4} \times \rho_{CH_4}) + n^l_{CH_4} + n^v_{water}} \tag{9}$$

Eq. 10 is the derivative of the solubility equation with respect to volume, v.

$$\frac{\partial x_i}{\partial v} = \frac{\rho_{CH_4}\left[\left(2 \times n^v_{EtOH}\right) + \left(2 \times n^v_{water}\right) + n^l_{EtOH} + n^l_{water}\right]}{\left[(v_{CH4} \times \rho_{CH_4}) + n^l_{CH_4} + n^v_{EtOH} + n^v_{water} + n^l_{EtOH} + n^l_{water}\right]^2} \tag{10}$$

Eq. 11 shows the solubility equation with respect to mass, m – CH_4 in methanol solution.

$$x_i = \frac{n^v_{CH_4} + \left[\left(n^l_{frac_{CH_4}} \times \frac{m}{32.04} \times wt\%\right) + \left(n^l_{frac_{CH_4}} \times \frac{m}{18} \times wt\%\right)\right] - \left[n^v_{MeOH} + n^v_{water}\right]}{n^v_{water} + \left(\frac{m}{32.04} \times wt\%\right) + \left(\frac{m}{18} \times wt\%\right) + n^v_{MeOH} + n^v_{CH_4} + \left[\left(n^l_{frac_{CH_4}} \times \frac{m}{32.04} \times wt\%\right) + \left(n^l_{frac_{CH_4}} \times \frac{m}{18} \times wt\%\right)\right]} \tag{11}$$

Eq. 12 shows the derivative of the solubility equation with respect to mass – 0.7 wt% MeOH.

$$\frac{\partial x_i}{\partial m} = \frac{-0.038 \times n^v_{CH_4} + n^v_{MeOH} \times \left(0.077 \times n^l_{frac_{CH_4}} + 0.038\right) + n^v_{water} \times \left(0.077 \times n^l_{frac_{CH_4}} + 0.038\right)}{\left[n^v_{CH_4} + \left(0.038 \times n^l_{frac_{CH_4}} \times m\right) + n^v_{MeOH} + n^v_{water} + 0.038m\right]^2} \tag{12}$$

Eq. 13 shows the solubility equation with respect to mass, m – CH_4 in ethanol solution.

$$x_i = \frac{n^v_{CH_4} + \left[\left(n^l_{frac_{CH_4}} \times \frac{m}{46} \times wt\%\right) + \left(n^l_{frac_{CH_4}} \times \frac{m}{18} \times wt\%\right)\right] - \left[n^v_{EtOH} + n^v_{water}\right]}{n^v_{water} + \left(\frac{m}{46} \times wt\%\right) + \left(\frac{m}{18} \times wt\%\right) + n^v_{EtOH} + n^v_{CH_4} + \left[\left(n^l_{frac_{CH_4}} \times \frac{m}{46} \times wt\%\right) + \left(n^l_{frac_{CH_4}} \times \frac{m}{18} \times wt\%\right)\right]} \quad (13)$$

Eq. 14 shows the derivative of the solubility equation with respect to mass – 0.7 wt% EtOH.

$$\frac{\partial x_i}{\partial m} = \frac{-0.032 \times n^v_{CH_4} + n^v_{EtOH} \times \left(0.064 \times n^l_{frac_{CH_4}} + 0.032\right) + n^v_{water} \times \left(0.064 \times n^l_{frac_{CH_4}} + 0.032\right)}{\left[n^v_{CH_4} + \left(0.032 \times n^l_{frac_{CH_4}} \times m\right) + n^v_{EtOH} + n^v_{water} + 0.032m\right]^2} \quad (14)$$

Eq. 15 shows the derivative of the solubility equation with respect to mass – 0.5 wt% EtOH.

$$\frac{\partial x_i}{\partial m} = \frac{-0.039 \times n^v_{CH_4} + n^v_{EtOH} \times \left(0.077 \times n^l_{frac_{CH_4}} + 0.039\right) + n^v_{water} \times \left(0.077 \times n^l_{frac_{CH_4}} + 0.039\right)}{\left[n^v_{CH_4} + \left(0.039 \times n^l_{frac_{CH_4}} \times m\right) + n^v_{EtOH} + n^v_{water} + 0.039m\right]^2} \quad (15)$$

Eq. 16 shows the solubility equation with respect to the mole fraction of CH_4 in liquid methanol/ethanol at atmospheric pressure.

$$x_i = \frac{n^v_{CH_4} + \left[n^{frac}_{CH_4} \times n^l_{EtOH}\right] + n^{water}_{CH_4} - \left[n^v_{EtOH} + n^v_{water}\right]}{\left[n^l_{EtOH} + n^v_{EtOH} + n^l_{water} + n^v_{water}\right] + \left[n^v_{CH_4} + n^{water}_{CH_4} + \left[n^{frac}_{CH_4} \times n^l_{EtOH}\right]\right]} \quad (16)$$

Eq. 17 shows the derivative of the equation with respect to the mole fraction of CH_4 in liquid methanol/ethanol at atmospheric pressure.

$$\frac{\partial x_i}{\partial n^{EtOH}_{CH_4}} = \frac{n^l_{EtOH} \times \left(n^l_{EtOH} + \left[2 \times n^v_{EtOH}\right] + \left[2 \times n^v_{water}\right] + n^l_{water}\right)}{\left[n^v_{CH_4} + \left(n^l_{EtOH} \times n^{frac}_{CH_4}\right) + n^l_{EtOH} + n^{water}_{CH_4} + n^v_{EtOH} + n^v_{water} + n^l_{water}\right]^2} \quad (17)$$

Eq. 18 shows the solubility equation with respect to the mole fraction of CH_4 in liquid methanol/ethanol at atmospheric pressure.

$$x_i = \frac{n_{CH_4}^{v} + \left[n_{CH_4}^{frac} \times n_{water}^{l} \right] + n_{CH_4}^{EtOH} - \left[n_{EtOH}^{v} + n_{water}^{v} \right]}{\left[n_{EtOH}^{l} + n_{EtOH}^{v} + n_{water}^{l} + n_{water}^{v} \right] + \left[n_{CH_4}^{v} + n_{CH_4}^{EtOH} + \left[n_{CH_4}^{frac} \times n_{water}^{l} \right] \right]} \qquad (18)$$

Eq. 19 shows the derivative of the equation with respect to the mole fraction of CH_4 in liquid water at atmospheric pressure.

$$\frac{\partial x_i}{\partial n_{CH_4}^{water}} = \frac{n_{water}^{l} \times \left(n_{water}^{l} + \left[2 \times n_{EtOH}^{v} \right] + \left[2 \times n_{water}^{v} \right] + n_{water}^{l} \right)}{\left[n_{CH_4}^{v} + \left(n_{water}^{l} \times n_{CH_4}^{frac} \right) + n_{water}^{l} + n_{CH_4}^{EtOH} + n_{EtOH}^{v} + n_{water}^{v} + n_{water}^{l} \right]^2} \qquad (19)$$

Eq. 20 shows the solubility equation with respect to the mole fraction of methanol/ethanol in gaseous CH_4 phase at atmospheric pressure.

$$x_i = \frac{n_{CH_4}^{v} + n_{CH_4}^{l} - \left[\left[n_{EtOH}^{frac} \times n_{v}^{CH_4} \right] + n_{water}^{v} \right]}{\left[n_{EtOH}^{l} + n_{water}^{l} \right] + \left[\left[n_{EtOH}^{frac} \times n_{CH_4}^{v} \right] + n_{water}^{v} \right] + \left[n_{CH_4}^{v} + n_{CH_4}^{l} \right]} \qquad (20)$$

Eq. 21 shows the derivative of the equation with respect to the mole fraction of methanol/ethanol in gaseous CH_4 phase at atmospheric pressure.

$$\frac{\partial x_i}{\partial n_{EtOH}^{frac}} = \frac{n_{CH_4}^{v} \times \left[\left(n_{CH_4}^{v} \times n_{CH_4}^{l} \right) + n_{CH_4}^{v} + n_{CH_4}^{l} + \left(2 \times n_{water}^{v} \right) + n_{EtOH}^{l} + n_{water}^{l} \right]}{\left[n_{CH_4}^{v} \times \left(n_{CH_4}^{l} + n_{EtOH}^{frac} \right) + n_{water}^{v} + n_{EtOH}^{l} + n_{water}^{l} \right]^2} \qquad (21)$$

Eq. 22 shows the solubility equation with respect to the mole fraction of ethanol in gaseous CH_4 phase at atmospheric pressure.

$$x_i = \frac{n_{CH_4}^{v} + n_{CH_4}^{l} - \left[\left[n_{water}^{frac} \times n_{v}^{CH_4} \right] + n_{EtOH}^{v} \right]}{\left[n_{EtOH}^{l} + n_{water}^{l} \right] + \left[\left[n_{water}^{frac} \times n_{CH_4}^{v} \right] + n_{EtOH}^{v} \right] + \left[n_{CH_4}^{v} + n_{CH_4}^{l} \right]} \qquad (22)$$

Eq. 23 shows the derivative of the equation with respect to the mole fraction of methanol/ethanol in gaseous CH_4 phase at atmospheric pressure.

$$\frac{\partial x_i}{\partial n_{water}^{frac}} = \frac{n_{CH_4}^{v} \times \left[\left(n_{CH_4}^{v} \times n_{CH_4}^{l} \right) + n_{CH_4}^{v} + n_{CH_4}^{l} + \left(2 \times n_{EtOH}^{v} \right) + n_{EtOH}^{l} + n_{water}^{l} \right]}{\left[n_{CH_4}^{v} \times \left(n_{CH_4}^{l} + n_{water}^{frac} \right) + n_{EtOH}^{v} + n_{EtOH}^{l} + n_{water}^{l} \right]^2} \quad (23)$$

Standard uncertainty in gas meter volume measurements, u(v) = 0.0005 L

Relative standard uncertainty in balance u_r(m) = 0.01 g

$u_r\left(n_{CH_4}^{frac}\right)$ = Relative standard uncertainty in CPA-SRK72 mole fraction calculation (optimized) of CH_4 in Liquid = 0.05

$u_r\left(n_{EtOH}^{frac}\right)$ = Relative standard uncertainty in CPA-SRK72 mole fraction calculation (optimized – limited data) of alcohol in CH_4 = 0.05

$u_r\left(n_{water}^{frac}\right)$ = Relative standard uncertainty in CPA-SRK72 mole fraction calculation (optimized – limited data) of water in CH_4 = 0.05

Standard uncertainty in NIST CH_4 density $u_r(\rho)$ = 0.0003 (deemed negligible)

The uncertainty in solvent composition, u(w) = 0.0001 (deemed negligible)

Standard uncertainty due to random error (repeatability), $u_{rep}(x_i)$ = 0.025

Eq. 24 standard uncertainty equation

$$u(x_i) = \sqrt{\begin{array}{l} \left(\frac{\partial x_i}{\partial v}^2 \times u(v)^2 + \left(\frac{\partial x_i}{\partial m}^2 \times u_r(m)^2 \right) + \left(\frac{\partial x_i}{\partial n_{CH_4}^{EtOH}}^2 \times u_r\left(n_{CH_4}^{EtOH}\right)^2 \right) + \ldots \right. \\ \left(\frac{\partial x_i}{\partial n_{CH_4}^{water}}^2 \times u_r\left(n_{CH_4}^{water}\right)^2 \right) + \left(\frac{\partial x_i}{\partial n_{EtOH}^{frac}}^2 \times u_r\left(n_{EtOH}^{frac}\right)^2 \right) + \ldots \\ \left. \left(\frac{\partial x_i}{\partial n_{water}^{frac}}^2 \times u_r\left(n_{water}^{frac}\right)^2 \right) + u_{rep}(x_i)^2 \right) \end{array}} \quad (24)$$

Table 8. Nomenclature for the uncertainty calculations.

x_i	Solubility of CH_4 in methanol/ethanol solution (mol frac)
$n_{CH_4}^{v}$	Mole of CH_4 in the vapor phase
$n_{CH_4}^{l}$	Mole of CH_4 in the liquid phase
n_{EtOH}^{v}	Mole of ethanol/methanol in the vapor phase
n_{EtOH}^{l}	Mole of Ethanol/Methanol in the liquid phase
v_{CH_4}	Volume of CH_4
ρ_{CH_4}	Density of CH_4
m_{EtOH}	Mass of ethanol/methanol
m_{water}	Mass of water
$n_{CH_4}^{frac}$	mole fraction of CH_4 in the alcohol calculated using the CPA-SRK72 EoS.
n_{EtOH}^{frac}	mole fraction of Ethanol/methanol in the CH_4 (gas meter) calculated using the CPA-SRK72
n_{water}^{frac}	mole fraction of water in the CH_4 (gas meter) calculated using the CPA-SRK72
$u_r(x_i)$	standard uncertainty [26]
$U_r(x_i)$	Expanded uncertainty
$u(v)$	Standard Uncertainty contribution by the gas meter volume as reported by the manufacturer
$u_r(m)$	Relative standard uncertainty contribution by the balance as reported by the manufacturer
$u_r(n_{CH_4}^{frac})$	Standard uncertainty contribution by the mole fraction CPA-SRK72 (optimized) calculation of CH_4 in the liquid phase
$u_r(n_{EtOH}^{frac})$	Standard uncertainty contribution by the mole fraction CPA-SRK72 (optimized – limited data) calculation of alcohol in the vapor phase

$u_r\left(n_{water}^{frac}\right)$	Standard uncertainty contribution by the mole fraction CPA-SRK72 (optimized – limited data) calculation of water in the vapor phase

AUTHOR INFORMATION

Corresponding Author

* Antonin Chapoy

Hydrates, Flow Assurance & Phase Equilibria, Institute of Petroleum Engineering, Heriot Watt University, EH14 4AS

Tel: +44 (0)131 451 3797

Fax: +44 (0)131 451 3539

Email: Antonin.chapoy@pet.hw.ac.uk

Present Addresses

* Hydrates, Flow Assurance & Phase Equilibria, Institute of Petroleum Engineering, Heriot Watt University, EH14 4AS

Author Contributions

The manuscript was written through contributions of all authors. All authors have given approval to the final version of the manuscript. These authors contributed equally.

Funding Sources

This project was funded through a Joint Industrial Project being conducted at the Institute of Petroleum Engineering, Heriot Watt University. The author would like to thank Chevron, GDF, Petrobras, Statoil and Total for their support of the project. I would also like to thank EPSRC for their support.

ACKNOWLEDGMENT

The author would like to thank Jim Allison, the team's technician, Dr. Jinhai Yang and SJ Hill for all the assistance provided.

References

(1) Kapateh, M. H.; Chapoy, A.; Burgass, R.; Tohidi, B. Experimental Measurement and Modeling of the Solubility of Methane in Methanol and Ethanol. *J. Chem. Eng. Data* **2015**, *61*, 666–673

(2) Wang, L.-K.; Chen, G.-J.; Han, G.-H.; Guo, X.-Q.; Guo, T.-M. Experimental study on the solubility of natural gas components in water with or without hydrate inhibitor. *Fluid Phase Equilib.* **2003**, *207*, 143–154.

(3) Yarym-agaev, N. .; Sinyavskaya R.P, K. фазовые равновесия в бинарных системах вода-метан, метанол-метан при высоких давлениях (Phase equilibria in binary systems of water-methane, methanol-methane at high pressures). *ZHurnal prikladoi Khimii* **1985**, *58*, 165–168.

(4) Brunner, E.; Hültenschmidt, W.; Schlichthärle, G. Fluid mixtures at high pressures IV. Isothermal phase equilibria in binary mixtures consisting of (methanol + hydrogen or nitrogen or methane or carbon monoxide or carbon dioxide). *J. Chem. Thermodyn.* **1987**, *19*, 273–291.

(5) Hong, J. H.; Malone, P. V.; Jett, M. D.; Kobayashi, R. The measurement and interpretation of the fluid-phase equilibria of a normal fluid in a hydrogen bonding solvent: the methane - methanol system. *Fluid Phase Equilib.* **1987**, *38*, 83–96.

(6) Schneider, R. PhD Thesis: Experimentelle Bestimmung der dynamischen Viskosität von Flüßigkeitsgemischen aus Methanol mit CO2, CH4, C2H6 und C3H8, Technical University of Berlin, 1978.

(7) Ukai, T.; Kodama, D.; Miyazaki, J.; Kato, M. Solubility of Methane in Alcohols and Saturated Density at 280.15 K. *J. Chem. Eng. Data* **2002**, *47*, 1320–1323.

(8) Frost, M.; Karakatsani, E.; von Solms, N.; Richon, D.; Kontogeorgis, G. M. Vapor–Liquid Equilibrium of Methane with Water and Methanol. Measurements and Modeling. *J. Chem. Eng. Data* **2014**, *59*, 961–967.

(9) Suzuki, K.; Sue, H.; Itou, M.; Smith, R. L.; Inomata, H.; Arai, K.; Saito, S. Isothermal vapor-liquid equilibrium data for binary systems at high pressures: carbon dioxide-methanol, carbon dioxide-ethanol, carbon dioxide-1-propanol, methane-ethanol, methane-1-propanol,

ethane-ethanol, and ethane-1-propanol systems. *J. Chem. Eng. Data* **1990**, *35*, 63–66.

(10) Brunner, E.; Hültenschmidt, W. Fluid mixtures at high pressures VIII. Isothermal phase equilibria in the binary mixtures: (ethanol + hydrogen or methane or ethane). *J. Chem. Thermodyn.* **1990**, *22*, 73–84.

(11) Friend, D. G.; Frurip, D. J.; Lemmon, E. W.; Morrison, R. E.; Olson, J. D.; Wilson, L. C. Establishing benchmarks for the Second Industrial Fluids Simulation Challenge. *Fluid Phase Equilib.* **2005**, *236*, 15–24.

(12) Lundstrøm, C.; Michelsen, M. L.; Kontogeorgis, G. M.; Pedersen, K. S.; Sørensen, H. Comparison of the SRK and CPA equations of state for physical properties of water and methanol. *Fluid Phase Equilib.* **2006**, *247*, 149–157.

(13) Zerpa, L. E.; Sloan, E. D.; Koh, C.; Sum, A. Hydrate Risk Assessment and Restart-Procedure Optimization of an Offshore Well Using a Transient Hydrate Prediction Model. *Oil Gas Facil.* **2012**, *1*, 49–56.

(14) Ferreira, P. A.; Bezerra, M. F. C.; Loschiavo, R. The Internal Corrosion Integrity Strategy on the Development of New Offshore Production Areas in Brazil. In *Offshore Technology Conference*; Offshore Technology Conference, 2013.

(15) Altoe Ferreira, P. The Internal Corrosion Integrity Strategy on the Development of New Offshore Production Areas in Brazil. *SPE Prod. Facil.* **2005**, *20*, 324–333.

(16) Chapoy, A.; Nazeri, M.; Kapateh, M.; Burgass, R.; Coquelet, C.; Tohidi, B. Effect of impurities on thermophysical properties and phase behaviour of a CO2-rich system in CCS. *Int. J. Greenh. Gas Control* **2013**, *19*, 92–100.

(17) Wise, M.; Chapoy, A. Carbon dioxide solubility in Triethylene Glycol and aqueous solutions. *Fluid Phase Equilib.* **2016**, *419*, 39–49.

(18) Haghighi, H.; Chapoy, A.; Burgess, R.; Mazloum, S.; Tohidi, B. Phase equilibria for petroleum reservoir fluids containing water and aqueous methanol solutions: Experimental measurements and modelling using the CPA equation of state. *Fluid Phase Equilib.* **2009**, *278*, 109–116.

(19) Haghighi, H.; Chapoy, A.; Burgess, R.; Tohidi, B. Experimental and thermodynamic modelling of systems containing water and ethylene glycol: Application to flow assurance

and gas processing. *Fluid Phase Equilib.* **2009**, *276*, 24–30.

(20) Anderson, R.; Chapoy, A.; Haghighi, H.; Tohidi, B. Binary Ethanol−Methane Clathrate Hydrate Formation in the System CH4-C2H5OH-H2O: Phase Equilibria and Compositional Analyses. *J. Phys. Chem. C* **2009**, *113*, 12602–12607.

(21) Kontogeorgis, G. M.; Voutsas, E. C.; Yakoumis, I. V.; Tassios, D. P. An Equation of State for Associating Fluids. *Ind. Eng. Chem. Res.* **1996**, *35*, 4310–4318.

(22) Soave, G. Equilibrium constants from a modified Redlich-Kwong equation of state. *Chem. Eng. Sci.* **1972**, *27*, 1197–1203.

(23) Michelsen, M. L.; Hendriks, E. M. Physical properties from association models. *Fluid Phase Equilib.* **2001**, *180*, 165–174.

(24) Chapoy, A.; Mohammadi, A. H.; Richon, D.; Tohidi, B. Gas solubility measurement and modeling for methane–water and methane–ethane–n-butane–water systems at low temperature conditions. *Fluid Phase Equilib.* **2004**, *220*, 111–119.

(25) Haghighi, H. PhD Thesis: Phase equilibria modelling of petroleum reservoir fluids containing water, Hydrate Inhibitors and Electrolyte Solutions, Heriot Watt University, Edinburgh, 2009.

(26) Taylor, B. N.; Kuyatt, C. E. *Guidelines for Evaluating and Expressing the Uncertainty of NIST Measurement Results*; 1994.

For Table of Contents Only